# The molecular basis of *Acinetobacter baumannii* cadmium toxicity and resistance

Saleh F. Alquethamy[1,2#], Felise G. Adams[3#], Ram Maharjan[4#], Natasha N. Delgado[4], Maoge Zang[3], James C. Paton[1], Karl A. Hassan[5], Ian T. Paulsen[4], Christopher A. McDevitt[1,2], Amy K. Cain[4], Bart A. Eijkelkamp[3*]

[1] Research Centre for Infectious Diseases, School of Biological Sciences, University of Adelaide, Adelaide, South Australia, Australia.

[2] Department of Microbiology and Immunology, The Peter Doherty Institute for Infection and Immunity, University of Melbourne, Melbourne, Victoria, Australia.

[3] College of Science and Engineering, Flinders University, Bedford Park, S.A., 5005, Australia

[4] ARC Centre of Excellence in Synthetic Biology, Department of Molecular Sciences, Macquarie University, Sydney, New South Wales, Australia.

[5] School of Environmental and Life Sciences, University of Newcastle, Callaghan, New South Wales, Australia.

[#]Saleh F. Alquethamy, Felise G. Adams and Ram Maharjan contributed equally to this work. Author order was determined by the time they joined the study.

College of Science and Engineering, Flinders University, Bedford Park, S.A., 5005, Australia. Phone: +61-8-8201-7779. E-mail: bart.eijkelkamp@flinders.edu.au.

Running Title: *A. baumannii* cadmium stress

**ABSTRACT**

*Acinetobacter* species are ubiquitous Gram-negative bacteria that can be found in water, soil and as commensals of the human skin. The successful inhabitation of *Acinetobacter* species in diverse environments is primarily attributable to the expression of an arsenal of stress resistance determinants, which includes an extensive repertoire of metal ion efflux systems. Although metal ion homeostasis in the hospital pathogen *Acinetobacter baumannii* is known to contribute to pathogenesis, insights into its metal ion transporters for environmental persistence are lacking. Here, we studied the impact of cadmium stress on *A. baumannii*. Our functional genomics and independent mutant analyses revealed a primary role for CzcE, a member of the cation diffusion facilitator (CDF) superfamily, in resisting cadmium stress. Further, we show that the CzcCBA heavy metal efflux system also contributes to cadmium efflux. Analysis of the *A. baumannii* metallome under cadmium stress showed zinc depletion and copper enrichment, which are likely to influence cellular fitness. Overall, this work expands our understanding of the role of membrane transporters in *A. baumannii* metal ion homeostasis.

**IMPORTANCE**

Cadmium toxicity is a widespread problem, yet the interaction of this heavy metal with biological systems is poorly understood. Some microbes have evolved traits to proactively counteract cadmium toxicity, which includes *Acinetobacter baumannii*. Here we show that *A. baumannii* utilises a dedicated cadmium efflux protein in concert with a system that is primarily attuned to zinc efflux, to efficiently overcome cadmium stress. The molecular characterization of *A. baumannii* under cadmium stress revealed how active cadmium efflux plays a key role in preventing the dysregulation of bacterial metal ion homeostasis, which appeared to be the primary means by which cadmium exerts toxicity upon the bacterium.

49 **INTRODUCTION**

50 The heavy metal cadmium is enriched in industrial settings and mining sites through
51 anthropogenic activity. Although various metalloproteins retain their function when bound to
52 cadmium (1), cadmium is primarily associated with toxicity in biological systems (2). Despite
53 being redox inactive, cadmium stress is commonly connected to the induction of oxidative
54 stress. Recent advances in the field have revealed cadmium-metalloprotein interactions as a
55 primary feature of cadmium toxicity (3, 4). In addition to dysregulation of central carbon
56 metabolism and lipid homeostasis, cadmium stress in *Streptococcus pneumoniae* causes
57 manganese and zinc starvation via interaction with non-cognate metalloproteins, these being a
58 manganese-recruiting protein and a zinc-responsive transcriptional regulator (4). Manganese is
59 the primary co-factor for superoxide dismutase in *S. pneumoniae*, hence, cadmium-induced
60 manganese depletion leads to oxidative stress susceptibility (4, 5). In *Salmonella enterica*,
61 excess cadmium was found to affect zinc and manganese accumulation, but not iron (3). These
62 studies exemplify that dysregulation of metal ion homeostasis and protein mismetallation by
63 cadmium is central to its toxicity in cells.

64

65 *Acinetobacter baumannii* is rapidly emerging as one of the world's most antimicrobial resistant
66 bacterial pathogens (6-8). Its highly effective intrinsic and acquired stress resistance features
67 have allowed this human pathogen to survive in the hospital environment, and thrive when
68 colonising immunocompromised individuals (9, 10). Various members of the *Acinetobacter*
69 genus, including some strains of *A. baumannii*, have a strong environmental presence. This has
70 resulted in the *A. baumannii* genome harbouring diverse metabolic and stress resistance
71 features that are typically not linked to pathogenicity (11, 12). Its environmental roots are also
72 reflected in the extensive arsenal of putative heavy metal export mechanisms that may enable
73 persistence under diverse metal ion stresses (13, 14). *A. baumannii* metal ion biology is a

74 rapidly expanding field of research. In particular its diverse array of metal ion acquisition
75 systems have been studied intently (15-21). In contrast, our understanding of heavy metal
76 resistance is limited, with only the roles of zinc and copper toxicity being studied in recent
77 years (13, 14, 22-24). Metal ion toxicity analyses in *A. baumannii* have revealed widespread
78 implications on cellular physiology, including dysregulation of metal ion homeostasis,
79 oxidative stress susceptibility and alterations in membrane biology. Similar to the impact of
80 cadmium on the dysregulation of *S. pneumoniae* and *S. enterica* metal ion homeostasis, zinc
81 stress in *A. baumannii* has been shown to result in copper depletion (13).
82
83 The *A. baumannii* genome harbours a broad arsenal of both highly-conserved and recently-
84 acquired efflux systems that have putative functions in metal resistance (13). The P-type
85 ATPase CopA has been shown to be the primary mediator of cytoplasmic copper efflux in *A.*
86 *baumannii* and plays a role in its virulence potential (23). The complexity of copper
87 homeostasis in the periplasm has also been studied (24), but strain-to-strain variation
88 complicates defining their significance across the species (13, 23). Zinc resistance is mediated
89 by an efficient efflux pathway which consists of the cation diffusion family (CDF) member
90 CzcD, a periplasmic zinc chaperone named CzcI and the heavy metal efflux (HME) system
91 CzcABC (22).
92
93 Bacterial cadmium efflux can be mediated by HME, CDF or P-type ATPase family members.
94 Examples include CadA, a P-type ATPase from *Streptococcus thermophilus* (25), the CDF
95 member YiiP from *Escherichia coli* (26, 27) and the CznABC HME system from *Helicobacter*
96 *pylori* (28). These systems may display overlapping substrate profiles within a bacterial
97 species, which requires experimental verification. Although a recent study has provided
98 insights into the role of the C-terminal domain in CDF metal specificity (29), overall, the

99 specificity for transition metals varies greatly between members within the CDF, HME and P-
100 type ATPase families and is difficult to predict based on protein sequence analyses.
101
102 In this study, we define the genome-wide cadmium stress adaptation mechanisms in *A.*
103 *baumannii*. This work identified both CDF and HME systems that play key roles in cadmium
104 export in *A. baumannii* which was confirmed by single-gene mutant analyses. We also show
105 that the bacterium encodes a highly efficient cadmium sensing regulator for the transcriptional
106 activation of the primary cadmium resistance mechanism. Through the global metallomic
107 analyses under cadmium stress, this study provides novel insights into cadmium toxicity.

108 **METHODS**

109 **Bacterial strains, chemicals, media and growth conditions**

110 *Acinetobacter baumannii* AB5075_UW mutant derivatives were purchased from the Manoil
111 Laboratory (30) and T26 transposon insertions confirmed by PCR. The *A. baumannii* ATCC
112 17978 *czcA* and *czcE* mutants were generated in our laboratory for a previous study (22) (See
113 **Tables S1** and **S2** for list of strains and oligonucleotides used in the study, respectively). All
114 chemicals were purchased from Sigma Aldrich (Australia) unless otherwise indicated.

115

116 *A. baumannii* strains were routinely grown in Luria Bertani broth (LB), containing 1% tryptone
117 (BD Bacto), 0.5% yeast extract (BD Bacto) and 0.5% sodium chloride. For overnight culturing,
118 a single colony from LB agar (1.5%) was used to inoculate 4 mL of LB medium. Overnight
119 cultures were diluted to an optical density at 600 nm ($OD_{600}$) of 0.01 in 200 µL LB for growth
120 assays or 20 mL LB for all other analyses. For growth assays, cultures in LB media were
121 incubated at 37°C with shaking in a FLUOstar Omega Spectrophotometer (BMG Labtech),
122 with the $OD_{600}$ values presented. The 20 mL cultures used for all other analyses were incubated
123 at 37°C in an Innova 40R shaking incubator (Eppendorf) at 230 rpm until they reached an
124 $OD_{600}$ of 0.7.

125

126 **Construction of transposon mutant library**

127 *A. baumannii* ATCC 17978 was used to generate a dense transposon library. The library was
128 constructed using the protocol as previously described (31). Briefly, transposomes were
129 prepared using an EZ-Tn*5* transposase (Epicentre Biotechnology) and a custom transposon
130 carrying a kanamycin resistance cassette amplified from the pUT_Km plasmid (32) using the
131 primer sets listed in **Table S2**. The transposomes (0.25 µL) were electroporated into 60 µL of
132 freshly prepared electrocompetent *A. baumannii* cells using a Bio-Rad GenePulser II (1.8 kV,

133 25 μF, and 200 Ω) in a 1 mm electrode gap cuvette (Bio-Rad). Cells were recovered by
134 resuspension in 1 mL of SOC medium and incubated at 37ºC with shaking (200 rpm) for 2 h.
135 Tn*5* insertion recombinants were selected on Mueller Hinton (MH) agar (BD Bacto)
136 supplemented with 7 $\mu g.mL^{-1}$ kanamycin. Approximately 12 to 16 transformations were
137 performed and pooled for each batch, with 10,000 to 50,000 resulting transformants.
138 Approximately 250,000 mutants were collected and pooled from a total of 10 batches and snap-
139 frozen and stored in 20% glycerol at -80ºC.
140
141 **Time kill assay for the selection of cadmium concentration for mutant library treatment**
142 Approximately $10^9$ CFU from an overnight ATCC 17978 culture was sub-cultured into fresh
143 10 mL MH broth spiked with different $CdCl_2$ concentrations (0, 3, 60, 80 160, and 320 μM)
144 and incubated at 37°C with shaking. At 0, 1, 2, 4, 5 and 24 h time points, 100 μL samples were
145 taken, 10-fold serially diluted in sterile phosphate-buffered saline (PBS) and 10 μL of each
146 dilution spotted on MH agar. Colonies were enumerated to determine the surviving cells after
147 overnight incubation at 37°C.
148
149 **Transposon-directed insertion site sequencing (TraDIS) of mutant library and data**
150 **analysis**
151 Approximately $10^9$ viable Tn*5* mutant cells were inoculated into 10 mL of MH broth (BD
152 Bacto) and grown at 37°C for 8 h with shaking (200 rpm). A total of 500 μL containing
153 approximately $10^9$ cells were seeded into 10 mL fresh MH broth with or without 60 μM $CdCl_2$
154 in duplicate and grown for 16 h at 37°C with shaking (200 rpm). Genomic DNA was then
155 extracted from approximately $10^{10}$ cells using the DNeasy UltraClean Microbial Kit (Qiagen)
156 according to the manufacture's protocol. Sequencing and analysis of the transposon mutant
157 library were performed using the transposon-directed insertion site sequencing (TraDIS)

158 protocol as described previously (33). The primer sets used for PCR amplification of TraDIS
159 fragments (Pf5_PCR) and sequencing (Pf5_Seq) are listed in **Table S2**. Samples were
160 sequenced on a HiSeq2500 Illumina sequencing platform, generating approximately 2 million
161 50 bp single-end reads per sample as previously described (34). TraDIS sequence reads were
162 deposited in the European Nucleotide Archive under accession number ERP118051 and
163 analysed using the BioTraDIS pipeline with default parameters (as described in (33)).
164
165 **Cellular metal ion content analysis**
166 Untreated and metal-stressed bacteria (LB supplemented with 1 μM $CdCl_2$ or 15 μM $CdCl_2$)
167 were harvested at mid log-phase ($OD_{600}$ 0.7) and washed, by resuspension and centrifugation
168 at 7,000 × *g* for 8 mins, first with PBS containing 5 mM ethylenediaminetetraacetic acid
169 (EDTA), and then with PBS as described previously (22, 23, 35, 36). Bacterial pellets were
170 desiccated at 95°C overnight, followed by determination of dry cell weight, and resuspension
171 of pellets in 35% $HNO_3$ and boiling at 95°C for 1 h. Samples were diluted to a final
172 concentration of 3.5% $HNO_3$ and analysed by inductively coupled plasma-mass spectrometry
173 (ICP-MS) on an Agilent Solution 8900 QQQ ICP-MS (Adelaide Microscopy, University of
174 Adelaide).
175
176 **qRT-PCR**
177 For RNA extraction and qRT-PCR analysis, untreated or metal-stressed bacteria (LB
178 supplemented with 30 μM $CdCl_2$) were harvested when they reached mid-log phase ($OD_{600}$
179 0.7) and cells lysed in QiaZol (Qiagen) as described previously (37, 38). RNA was extracted
180 and purified using a PureLink RNA Mini Kit (ThermoFisher Scientific), with on-column
181 DNase I treatment, according to the manufacturer's instructions. qRT-PCR was performed
182 using the SuperScript III One-Step RT-PCR kit (ThermoFisher Scientific) on a QuantStudio 7

183 Flex System (ThermoFisher Scientific). Transcription levels were corrected to those obtained
184 for *GAPDH* prior to normalization to the transcription levels observed for untreated *A.*
185 *baumannii* cultures. Oligonucleotide sequences are listed in (**Table S2**).
186
187 **Bacterial lipid extraction and gas chromatography/mass spectrometry analysis**
188 Overnight cultures of *A. baumannii* AB5075_UW were diluted to an $OD_{600}$ of 0.05 in fresh LB
189 media (20 ml) and grown to mid-log phase ($OD_{600}$ = 0.7), with treated cultures supplemented
190 with 15 µM $CdCl_2$. Cells were harvested by centrifugation at 7,000 × *g* for 10 minutes and
191 washed once with PBS, processed pellets were then resuspended in 50 µl of 1.5% NaCl buffer.
192 For lipid extraction, 1 ml of chloroform:methanol (2:1; v/v) was added to the cell suspension,
193 mixed vigorously for 2 minutes then incubated at RT for 10 minutes. Following the addition
194 of 200 µl 1.5% NaCl, the cell suspension was mixed vigorously for 1 minute and centrifuged
195 at 6,000 × *g* for phase-separation. The lower phase was recovered and concentrated via nitrogen
196 evaporation. All samples were stored at -20ºC prior to gas chromatography / mass spectrometry
197 (GC/MS) analysis.
198
199 To generate fatty acid methyl esters (FAMEs), concentrated lipid samples were resuspended in
200 1:1 chloroform and trimethylsulfonium hydroxide (TMSOH) and subsequently analysed using
201 an Agilent 7890A GC system with a 30 m Agilent DB-FastFAME column (Agilent
202 Technologies). Mass spectrometry was completed using a coupled Agilent 5975C MSD system
203 (Agilent Technologies). FAME species were differentiated and determined by comparing to
204 the FAME mix c4-24 standard (Sigma Aldrich). Data analysis was completed using the Agilent
205 MassHunter Qualitative Navigator software (Agilent Technologies).

206 **RESULTS AND DISCUSSION**

207 ***A. baumannii* employs multiple transport systems to resist cadmium stress**

208 To delineate the molecular basis of cadmium toxicity and the mechanisms that aid in cadmium
209 stress resistance we created a Tn*5*-based random transposon mutant library in the laboratory
210 reference strain, *A. baumannii* ATCC 17978. TraDIS sequencing of the base library in rich
211 media revealed a density of at least 113,000 unique mutants. We subjected $10^9$ mutant cells to
212 a subinhibitory concentration (60 μM) of cadmium for 16 h. This concentration was found to
213 present a minor but significant impact on proliferation of this strain (**Fig. S1**), and thus deemed
214 appropriate for TraDIS analysis. Cadmium exposure resulted in 56 genes displaying
215 significantly differential numbers of insertions (**Table S3**): decreased mutant fitness (decreased
216 transposon insertions) in 14 genes and enhanced fitness (increased transposon insertions) in 42
217 genes (fold change of ≥ 2; *Q* value, ≤ 0.05).

218

219 The TraDIS analyses identified ACX60_13165, which encodes a putative MerR-like
220 transcriptional regulator, as most affected by cadmium treatment (-4.1 fold change) (**Fig. 1**).
221 The regulatory gene is divergently transcribed to the CDF family transport gene, *czcE*
222 (ACX60_13160), which our analyses defined as the gene with the second greatest loss of
223 represented transposon mutants under cadmium stress (-3.8 fold change). The previously
224 characterized HME-RND zinc efflux system, CzcCBA (ACX60_01405-15) and its metal
225 chaperone *czcI* (ACX60_01400) (22), were also shown to be important in conferring cadmium
226 resistance, where mutant abundance decreased between -2.4 and -3.0 fold change. The CDF
227 member, *czcD*, previously revealed to play a role in zinc efflux, was not found to be
228 significantly impacted by cadmium treatment. We identified that transposon mutants of
229 putative DmeF-like cobalt exporting CDF (ACX60_18165) were enriched under cadmium
230 stress (2.1 fold change). This indicates that cobalt may be accumulated at reduced levels under

231 cadmium stress and its undesired export by this DmeF-like transporter is subsequently
232 detrimental to *A. baumannii* fitness.
233
234 A solute binding protein (SBP; ACX60_10710) with similarity to methionine and metal ion
235 binding SBPs such as NlpA (COG1464.1), was impacted by cadmium stress (-3.2 fold change).
236 The gene encoding this periplasmic protein is located in an operon that also encodes its putative
237 ATP-binding cassette (ABC) transporter for cargo delivery and subsequent translocation across
238 the inner membrane, but none of these genes were affected by cadmium stress. Hence, the SBP
239 may play a role in periplasmic metal buffering instead of facilitating transport.
240
241 The relatively large number of genes in which insertional disruption proved to impart a positive
242 effect included various transcriptional regulators. H-NS (12.6 fold change) is one of *A.*
243 *baumannii*'s most prominent global transcriptional regulators (39). Although, no role in metal
244 ion stress has been indicated in previous transcriptomic analyses of an ATCC 17978 *hns*
245 mutant, in *Salmonella*, the ferric uptake regulator (FUR) regulates the expression of *hns* and
246 H-NS competes with FUR for some gene targets in *Salmonella* (40, 41). The GacAS regulatory
247 system, of which mutation is beneficial to survival during cadmium stress (11.7 and 12.1 fold
248 change, respectively), plays a key role during infection and in lifestyle changes, including
249 biofilm formation (42). Other regulators include those with putative roles in sensing saturated
250 fatty acids, including ACX60_05275 (3.3 fold change) and ACX60_17890 (2.0 fold change).
251 This may indicate that *A. baumannii* adapts to cadmium stress by changing the structure and
252 subsequently the biophysical properties of its membrane. Fatty acid analysis of *A. baumannii*
253 under cadmium stress revealed minor but significant changes in 16:1 (1.5% decrease) and 18:0
254 (0.9% increase) (**Fig. S2**). These changes may indicate a slight increase in the membrane
255 rigidity following cadmium exposure.

256

257 ***A. baumannii* employs a dedicated inner membrane cadmium exporter**

258 To confirm the roles of the putative cadmium transporters in cadmium stress resistance as
259 observed by TraDIS (**Fig. S3**), we examined mutants in *czcA* (ABUW_0268), *czcD*
260 (ABUW_0269), *czcE* (ABUW_2851) and *czcF* (ABUW_3664). *A. baumannii* AB5075_UW
261 and its mutant derivatives were grown with increasing concentrations of cadmium (1, 5, 10, 20
262 or 30 μM $CdCl_2$) (**Fig. 2A-E**). We found that inactivation of *czcE* rendered the cells hyper-
263 susceptible to cadmium stress, with significant growth perturbation seen at concentrations as
264 low as 1 μM cadmium, which is approximately 30-fold lower than the AB5075_UW parental
265 strain. In addition to a primary role in zinc resistance (22), CzcCBA contributes to cadmium
266 resistance, with the *czcA*::T26 mutant showing increased sensitivity at 20 μM cadmium or
267 greater. Consistent with the examination of these efflux systems in strain AB50875_UW, the
268 ATCC 17978 Δ*czcA* and Δ*czcE* mutants displayed increased susceptibility to cadmium stress
269 (**Fig. S4**). CzcD and CzcF were found not to play a major role in cadmium resistance. The
270 concerted efforts from this study and previous work (22) have identified major roles for CzcA,
271 CzcD and CzcE in zinc and/or cadmium resistance, but no major role has been identified for
272 CzcF. Hence, we examined the response of CzcF to stress induced by other transition metals
273 (zinc, copper, nickel, cobalt and iron), which revealed a minor role in zinc and nickel resistance
274 (**Fig. S5**).

275

276 **The impact of cadmium on the *A. baumannii* metallome**

277 Bacterial cells necessitate diligent balancing of metal ions as their hyper-accumulation or
278 deficit beyond the cellular setpoints has detrimental impacts on metalloprotein function and
279 has the potential to affect the homeostasis of other metals. First, we examined cadmium
280 accumulation in *A. baumannii* strain AB5075_UW and the *czcA*::T26 and *czcE*::T26 mutant

281 strains. These analyses revealed that CzcA inactivation did not impact accumulation following
282 supplementation with 1 μM cadmium. In contrast, the *czcE*::T26 mutant accumulated cadmium
283 at nearly 8-fold higher levels compared to the wild-type (**Fig. 3A**). Since growth of the
284 *czcE*::T26 mutant was dramatically perturbed at concentrations greater than 1 μM cadmium,
285 only the wild-type and *czcA*::T26 mutant were examined at 15 μM cadmium. The *czcA*::T26
286 mutant accumulated cadmium at greater levels than those observed for the wild-type (144 vs.
287 86 μg cadmium.g cells$^{-1}$) (**Fig. 3A**).
288
289 Examination of the impact of cadmium on the most abundant *A. baumannii* metal ions revealed
290 that zinc and copper levels were affected, but not iron (**Fig. 3B-D**). Zinc levels in the wild-type
291 were significantly lower upon exposure to 1 μM cadmium and below detection when exposed
292 to 15 μM cadmium. Consistent with these findings, zinc levels in the *czcA*::T26 and *czcA*::T26
293 mutants decreased to a greater extent upon exposure to 1 μM cadmium compared to the wild-
294 type (**Fig. 3B**). Interestingly, the wild-type and *czcA*::T26 mutant hyper-accumulated copper
295 when exposed to 15 μM cadmium (**Fig. 3D**). Despite the similar cellular cadmium levels
296 observed in the *czcE*::T26 mutant following treatment with 1 μM cadmium and the wild-type
297 with 15 μM cadmium (**Fig. 2A**), the accumulation of copper was not affected in the *czcE*::T26
298 mutant (**Fig. 2D**).
299
300 **Cadmium stress influences the *A. baumannii* metalloregulator responses**
301 Transcriptional analyses revealed that *czcE* is up-regulated 480-fold by cadmium stress (**Fig.**
302 **4A**), while *czcI* was significantly down-regulated by cadmium stress. Analysis of CadR
303 (ABUW_2852), a MerR-type regulator divergently transcribed from *czcE*, suggested that it
304 was responsible for activation of *czcE*, which is consistent with the TraDIS analysis (**Fig. 4B**).
305 We found that *czcF* was significantly up-regulated upon treatment with cadmium, despite it

306 not playing a major role in cadmium resistance (**Fig. 4I and S6B**). Similar to *czcE*, we found
307 that *czcF* is regulated by a divergently transcribed MerR-type regulator, ABUW_3665 (**Fig.**
308 **4C**).
309
310 Our metallomic analyses identified that cadmium toxicity impacts zinc and copper homeostasis
311 (**Fig. 2**). To ascertain the impact of cadmium stress on the expression of metal ion homeostasis
312 contributors, we analysed transcription of *znuA*, a component of the major zinc acquisition
313 system ZnuABC (15), *oprC*, a putative copper acquisition system (43), and *copA*, the primary
314 copper efflux system (22). Under cadmium stress, *A. baumannii* increases expression of *znuA*
315 (3.3 $\log_2$-fold) (**Fig. 4D**), possibly in an attempt to compensate for zinc starvation. Interestingly,
316 cadmium-induced copper overaccumulation may be a result of the significant up-regulation of
317 *oprC* (8.2 $\log_2$-fold) (**Fig. 4D**).

318 **CONCLUSION**

319 Cadmium resistance in *A. baumannii* is primarily mediated by a distinct CDF member, CzcE.
320 However, mutation of *czcA* results in *A. baumannii* growth perturbation in the presence of
321 cadmium, which suggests that cytoplasmic cadmium is translocated into the periplasm by CzcE
322 and then exported into the extracellular space by CzcCBA. These findings on the roles of CDFs
323 in conjunction with HME systems in the cytoplasmic and periplasmic translocation of
324 substrates, respectively, are consistent with work performed with *Wautersia metallidurans*
325 (44). Further, previous works have indicated that cadmium exerts greater toxicity in the
326 cytoplasm compared to that of the periplasm (45, 46), which highlights the major significance
327 of CzcE, and the lesser contribution of CzcA in *A. baumannii* cadmium resistance.
328 Interestingly, transcriptional profiling revealed that *czcE* is transcriptionally activated by
329 cadmium, whereas *czcA* transcription is not. Hence, the degree of CzcCBA contribution to
330 cadmium resistance may also be due to the lack of up-regulation, rather than an inability of
331 export from either the cytoplasm or periplasm.

332

333 Cadmium stress also results in copper over-accumulation with transcriptional analyses
334 revealing *oprC* to be a possible copper import system. Although *oprC* has been shown to be
335 regulated by OxyR in *Acinetobacter oleivorans* (47), recent analyses of OxyR in *A. baumannii*
336 did not identify such association (48). Hence, the physiological role of OprC warrants further
337 investigation. Zinc homeostasis was also affected by cadmium stress, resulting in a reduction
338 in cellular zinc. However, the molecular basis behind cadmium-induced zinc depletion in *A.*
339 *baumannii* remains unclear. These results show that cadmium stress results in an inverse
340 dysregulation of copper and zinc homeostasis, which at is at least in part consistent with our
341 previous analysis of these metals (13).

342

343 In summary, this study has identified the primary cadmium efflux pathways of *A. baumannii*.
344 These systems are highly conserved across this species and genus, hence this work is broadly
345 applicable to *Acinetobacter* biology, exemplified by our parallel analysis of two distinct strains.
346 We have garnered new knowledge into the environmental stress adaptation strategies, with
347 systems that have unique and shared metal ion specificities. The analyses of cadmium stress
348 across a range of distinct metal ion export systems has also provided novel insights into the
349 alignment of metal sensors and efflux systems, which is of major significance to bacterial
350 fitness in a broad range of environments.

**Funding**

This work was supported by the National Health and Medical Research Council (Australia) through Project Grant 1159752 to BAE and AKC. AKC was supported by an Australian Research Council (ARC) DECRA fellowship (DE180100929), CAM is an ARC Future Fellow (FT170100006) and KAH is an ARC Future Fellow (FT180100123).

**Authors' contributions**

BAE, KAH, AKC, ITP, JCP and CAM designed the study. SFA, FGA, RM, KAH, NND and BAE performed the experiments. BAE, FGA, SFA, KAH, AKC, RM, ITP, CAM and JCP contributed to the drafting of the manuscript.

361 **REFERENCES**


362 1. Malgieri G, Palmieri M, Esposito S, Maione V, Russo L, Baglivo I, de Paola I, Milardi
363 D, Diana D, Zaccaro L, Pedone PV, Fattorusso R, Isernia C. 2014. Zinc to cadmium
364 replacement in the prokaryotic zinc-finger domain. Metallomics 6:96-104.

365 2. Dietrich N, Tan CH, Cubillas C, Earley BJ, Kornfeld K. 2016. Insights into zinc and
366 cadmium biology in the nematode *Caenorhabditis elegans*. Arch Biochem Biophys
367 611:120-133.

368 3. Ammendola S, Cerasi M, Battistoni A. 2014. Deregulation of transition metals
369 homeostasis is a key feature of cadmium toxicity in Salmonella. Biometals 27:703-14.

370 4. Begg SL, Eijkelkamp BA, Luo Z, Counago RM, Morey JR, Maher MJ, Ong CL,
371 McEwan AG, Kobe B, O'Mara ML, Paton JC, McDevitt CA. 2015. Dysregulation of
372 transition metal ion homeostasis is the molecular basis for cadmium toxicity in
373 *Streptococcus pneumoniae*. Nat Commun 6:6418.

374 5. Eijkelkamp BA, Morey JR, Ween MP, Ong CL, McEwan AG, Paton JC, McDevitt CA.
375 2014. Extracellular zinc competitively inhibits manganese uptake and compromises
376 oxidative stress management in *Streptococcus pneumoniae*. PLoS One 9:e89427.

377 6. WHO. 2017. WHO publishes list of bacteria for which new antibiotics are urgently
378 needed. WHO Media centre.

379 7. Tacconelli E, Carrara E, Savoldi A, Harbarth S, Mendelson M, Monnet DL, Pulcini C,
380 Kahlmeter G, Kluytmans J, Carmeli Y, Ouellette M, Outterson K, Patel J, Cavaleri M,
381 Cox EM, Houchens CR, Grayson ML, Hansen P, Singh N, Theuretzbacher U, Magrini
382 N, Group WHOPPLW. 2018. Discovery, research, and development of new antibiotics:
383 the WHO priority list of antibiotic-resistant bacteria and tuberculosis. Lancet Infect Dis
384 18:318-327.

385 8. CDC. 2019. 2019 Antibiotic Resistance Threats Report. CDC.

386 9. Cerqueira GM, Peleg AY. 2011. Insights into *Acinetobacter baumannii* pathogenicity.
387 IUBMB Life 63:1055-60.

388 10. Peleg AY, de Breij A, Adams MD, Cerqueira GM, Mocali S, Galardini M, Nibbering
389 PH, Earl AM, Ward DV, Paterson DL, Seifert H, Dijkshoorn L. 2012. The success of
390 acinetobacter species; genetic, metabolic and virulence attributes. PLoS One 7:e46984.

391 11. Adams MD, Goglin K, Molyneaux N, Hujer KM, Lavender H, Jamison JJ, MacDonald
392 IJ, Martin KM, Russo T, Campagnari AA, Hujer AM, Bonomo RA, Gill SR. 2008.
393 Comparative genome sequence analysis of multidrug-resistant *Acinetobacter*
394 *baumannii*. J Bacteriol 190:8053-64.

395 12. Farrugia DN, Elbourne LD, Hassan KA, Eijkelkamp BA, Tetu SG, Brown MH, Shah
396 BS, Peleg AY, Mabbutt BC, Paulsen IT. 2013. The complete genome and phenome of
397 a community-acquired *Acinetobacter baumannii*. PLoS One 8:e58628.

398 13. Hassan KA, Pederick VG, Elbourne LD, Paulsen IT, Paton JC, McDevitt CA,
399 Eijkelkamp BA. 2017. Zinc stress induces copper depletion in Acinetobacter
400 baumannii. BMC Microbiol 17:59.

401 14. Williams CL, Neu HM, Gilbreath JJ, Michel SL, Zurawski DV, Merrell DS. 2016.
402 Copper resistance of the emerging pathogen *Acinetobacter baumannii*. Appl Environ
403 Microbiol 82:6174-6188.

404 15. Hood MI, Mortensen BL, Moore JL, Zhang Y, Kehl-Fie TE, Sugitani N, Chazin WJ,
405 Caprioli RM, Skaar EP. 2012. Identification of an *Acinetobacter baumannii* zinc
406 acquisition system that facilitates resistance to calprotectin-mediated zinc
407 sequestration. PLoS Pathog 8:e1003068.

408 16. Mortensen BL, Rathi S, Chazin WJ, Skaar EP. 2014. *Acinetobacter baumannii* response
409 to host-mediated zinc limitation requires the transcriptional regulator Zur. J Bacteriol
410 196:2616-26.

411 17. Nairn BL, Lonergan ZR, Wang J, Braymer JJ, Zhang Y, Calcutt MW, Lisher JP, Gilston
412 BA, Chazin WJ, de Crecy-Lagard V, Giedroc DP, Skaar EP. 2016. The response of
413 *Acinetobacter baumannii* to zinc starvation. Cell Host Microbe 19:826-36.

414 18. Gaddy JA, Arivett BA, McConnell MJ, Lopez-Rojas R, Pachon J, Actis LA. 2012. Role
415 of acinetobactin-mediated iron acquisition functions in the interaction of *Acinetobacter*

416 *baumannii* strain ATCC 19606T with human lung epithelial cells, *Galleria mellonella*
417 caterpillars, and mice. Infect Immun 80:1015-24.

418 19. Nwugo CC, Gaddy JA, Zimbler DL, Actis LA. 2011. Deciphering the iron response in
419 *Acinetobacter baumannii*: A proteomics approach. J Proteomics 74:44-58.

420 20. Zimbler DL, Penwell WF, Gaddy JA, Menke SM, Tomaras AP, Connerly PL, Actis
421 LA. 2009. Iron acquisition functions expressed by the human pathogen *Acinetobacter*
422 *baumannii*. Biometals 22:23-32.

423 21. Eijkelkamp BA, Hassan KA, Paulsen IT, Brown MH. 2011. Investigation of the human
424 pathogen *Acinetobacter baumannii* under iron limiting conditions. BMC Genomics
425 12:126.

426 22. Alquethamy SF, Adams FG, Naidu V, Khorvash M, Pederick VG, Zang M, Paton JC,
427 Paulsen IT, Hassan KA, Cain AK, McDevitt CA, Eijkelkamp BA. 2020. The role of
428 zinc efflux during *Acinetobacter baumannii* infection. ACS Infect Dis 6:150-158.

429 23. Alquethamy SF, Khorvash M, Pederick VG, Whittall JJ, Paton JC, Paulsen IT, Hassan
430 KA, McDevitt CA, Eijkelkamp BA. 2019. The role of the CopA copper efflux system
431 in *Acinetobacter baumannii* virulence. Int J Mol Sci 20.

432 24. Williams CL, Neu HM, Alamneh YA, Reddinger RM, Jacobs AC, Singh S, Abu-Taleb
433 R, Michel SLJ, Zurawski DV, Merrell DS. 2020. Characterization of *Acinetobacter*
434 *baumannii* copper resistance reveals a role in virulence. Front Microbiol 11:16.

435 25. Schirawski J, Hagens W, Fitzgerald GF, Van Sinderen D. 2002. Molecular
436 characterization of cadmium resistance in *Streptococcus thermophilus* strain 4134: an
437 example of lateral gene transfer. Appl Environ Microbiol 68:5508-16.

438 26. Lu M, Fu D. 2007. Structure of the zinc transporter YiiP. Science 317:1746-8.

439 27. Wei Y, Fu D. 2006. Binding and transport of metal ions at the dimer interface of the
440 Escherichia coli metal transporter YiiP. J Biol Chem 281:23492-502.

441 28. Stahler FN, Odenbreit S, Haas R, Wilrich J, Van Vliet AH, Kusters JG, Kist M,
442 Bereswill S. 2006. The novel *Helicobacter pylori* CznABC metal efflux pump is

443 required for cadmium, zinc, and nickel resistance, urease modulation, and gastric
444 colonization. Infect Immun 74:3845-52.

445 29. Udagedara SR, La Porta DM, Spehar C, Purohit G, Hein MJA, Fatmous ME, Casas
446 Garcia GP, Ganio K, McDevitt CA, Maher MJ. 2020. Structural and functional
447 characterizations of the C-terminal domains of CzcD proteins. J Inorg Biochem
448 208:111087.

449 30. Gallagher LA, Ramage E, Weiss EJ, Radey M, Hayden HS, Held KG, Huse HK,
450 Zurawski DV, Brittnacher MJ, Manoil C. 2015. Resources for genetic and genomic
451 analysis of emerging pathogen *Acinetobacter baumannii*. J Bacteriol 197:2027-35.

452 31. Langridge GC, Phan MD, Turner DJ, Perkins TT, Parts L, Haase J, Charles I, Maskell
453 DJ, Peters SE, Dougan G, Wain J, Parkhill J, Turner AK. 2009. Simultaneous assay of
454 every Salmonella Typhi gene using one million transposon mutants. Genome Res
455 19:2308-16.

456 32. Herrero M, de Lorenzo V, Timmis KN. 1990. Transposon vectors containing non-
457 antibiotic resistance selection markers for cloning and stable chromosomal insertion of
458 foreign genes in gram-negative bacteria. J Bacteriol 172:6557-67.

459 33. Barquist L, Mayho M, Cummins C, Cain AK, Boinett CJ, Page AJ, Langridge GC,
460 Quail MA, Keane JA, Parkhill J. 2016. The TraDIS toolkit: sequencing and analysis for
461 dense transposon mutant libraries. Bioinformatics 32:1109-11.

462 34. Hassan KA, Cain AK, Huang T, Liu Q, Elbourne LD, Boinett CJ, Brzoska AJ, Li L,
463 Ostrowski M, Nhu NT, Nhu Tdo H, Baker S, Parkhill J, Paulsen IT. 2016.
464 Fluorescence-Based Flow Sorting in Parallel with Transposon Insertion Site
465 Sequencing Identifies Multidrug Efflux Systems in Acinetobacter baumannii. MBio 7.

466 35. Pederick VG, Eijkelkamp BA, Begg SL, Ween MP, McAllister LJ, Paton JC, McDevitt
467 CA. 2015. ZnuA and zinc homeostasis in *Pseudomonas aeruginosa*. Sci Rep 5:13139.

468 36. Eijkelkamp BA, Begg SL, Pederick VG, Trapetti C, Gregory MK, Whittall JJ, Paton
469 JC, McDevitt CA. 2018. Arachidonic acid stress impacts Pneumococcal fatty acid
470 homeostasis. Front Microbiol 9:813.

471 37. Hassan KA, Jackson SM, Penesyan A, Patching SG, Tetu SG, Eijkelkamp BA, Brown
472 MH, Henderson PJ, Paulsen IT. 2013. Transcriptomic and biochemical analyses
473 identify a family of chlorhexidine efflux proteins. Proc Natl Acad Sci U S A 110:20254-
474 9.

475 38. Giles SK, Stroeher UH, Eijkelkamp BA, Brown MH. 2015. Identification of genes
476 essential for pellicle formation in *Acinetobacter baumannii*. BMC Microbiol 15:116.

477 39. Eijkelkamp BA, Stroeher UH, Hassan KA, Elbourne LD, Paulsen IT, Brown MH. 2013.
478 H-NS plays a role in expression of *Acinetobacter baumannii* virulence features. Infect
479 Immun 81:2574-83.

480 40. Prajapat MK, Saini S. 2012. Interplay between Fur and HNS in controlling virulence
481 gene expression in Salmonella typhimurium. Comput Biol Med 42:1133-40.

482 41. Troxell B, Sikes ML, Fink RC, Vazquez-Torres A, Jones-Carson J, Hassan HM. 2011.
483 Fur negatively regulates hns and is required for the expression of HilA and virulence in
484 *Salmonella enterica* serovar Typhimurium. J Bacteriol 193:497-505.

485 42. Cerqueira GM, Kostoulias X, Khoo C, Aibinu I, Qu Y, Traven A, Peleg AY. 2014. A
486 global virulence regulator in *Acinetobacter baumannii* and its control of the
487 phenylacetic acid catabolic pathway. J Infect Dis 210:46-55.

488 43. Abdollahi S, Rasooli I, Mousavi Gargari SL. 2018. The role of TonB-dependent copper
489 receptor in virulence of *Acinetobacter baumannii*. Infect Genet Evol 60:181-190.

490 44. Munkelt D, Grass G, Nies DH. 2004. The chromosomally encoded cation diffusion
491 facilitator proteins DmeF and FieF from *Wautersia metallidurans* CH34 are
492 transporters of broad metal specificity. J Bacteriol 186:8036-43.

493 45. Helbig K, Bleuel C, Krauss GJ, Nies DH. 2008. Glutathione and transition-metal
494 homeostasis in *Escherichia coli*. J Bacteriol 190:5431-8.

495 46. Helbig K, Grosse C, Nies DH. 2008. Cadmium toxicity in glutathione mutants of
496 *Escherichia coli*. J Bacteriol 190:5439-54.

497 47. Kim J, Cho Y, Jang IA, Park W. 2015. Molecular mechanism involved in the response
498 to hydrogen peroxide stress in *Acinetobacter oleivorans* DR1. Appl Microbiol
499 Biotechnol 99:10611-26.

500 48. Juttukonda LJ, Green ER, Lonergan ZR, Heffern MC, Chang CJ, Skaar EP. 2018.
501 *Acinetobacter baumannii* OxyR regulates the transcriptional response to hydrogen
502 peroxide. Infect Immun doi:10.1128/IAI.00413-18.

503

504 **FIGURE LEGENDS**

505 **Figure 1. The *A. baumannii* cadmium resistome.** The effect of cadmium treatment (60 μM
506 for 16 hours) on the abundance of gene mutations (Tn*5* insertions) mapping to the *A. baumannii*
507 ATCC 17978 chromosome and plasmid pAB3 as determined by TraDIS analysis. The data
508 represent the mean of biological triplicates. The *Q* value was determined by using the method
509 described previously (33).

510

511 **Figure 2. Cadmium resistance in *A. baumannii*.** The effects of cadmium (1, 5, 10, 20 or 30
512 μM $CdCl_2$) upon growth of the **(A)** wild-type, **(B)** *czcA*::T26, **(C)** *czcD*::T26, **(D)** *czcE*::T26 or
513 **(E)** *czcF*::T26 mutant cells was compared to that of untreated (UT) cells. The growth was
514 examined by measuring the optical density at 600 nm ($OD_{600}$). The data are the mean of at least
515 biological triplicates (± SEM). The visibility of error bars may be occluded by the symbols.

516

517 **Figure 3. The impact of cadmium exposure on *A. baumannii* metal ion homeostasis.** The
518 accumulation of **(A)** cadmium, **(B)** iron, **(C)** zinc and **(D)** copper in wild-type, *czcA*::T26 or
519 *czcE*::T26 cells with or without cadmium supplementation (1 μM or 15 μM $CdCl_2$), as
520 determined by inductively coupled plasma – mass spectrometry. Metal ion levels were
521 quantified as the weight of the metal (μg) per the weight of the dry cell pellet (g). For all panels,
522 the data are the mean of at least biological triplicates (± SEM). Statistical analyses were
523 performed using a two-tailed Student's *t*-test; n.s. = not significant, * = $p < 0.05$, ** = $p < 0.01$
524 and **** = $p < 0.0001$. The detection limit of zinc is indicated by the dotted line (b.d. = below
525 detection).

526

527 **Figure 4. Regulation of cadmium resistance. (A)** The transcriptional responses of *czcI*, *czcC*,
528 *czcA*, *czcD*, *czcE* and *czcF* in wild-type AB5075_UW cells treated with 30 μM cadmium were

529 examined by qRT-PCR. The transcription levels of **(B)** *czcE* or **(C)** *czcF* were examined in
530 regulator mutant and AB5075_UW wild-type cells by qRT-PCR following treatment with 30
531 μM cadmium. **(D)** The transcription levels of *znuA*, *oprC* and *copA* in wild-type cells were
532 examined by qRT-PCR following treatment with 30 μM cadmium. For all panels, the data are
533 the mean (±SEM) of at least biological triplicates. The visibility of error bars may be occluded
534 by the symbols. Statistical analyses were performed using a two-tailed Student *t*-test; n.s. = not
535 significant, * = $p < 0.05$, ** = $p < 0.01$ and *** = $p < 0.001$.

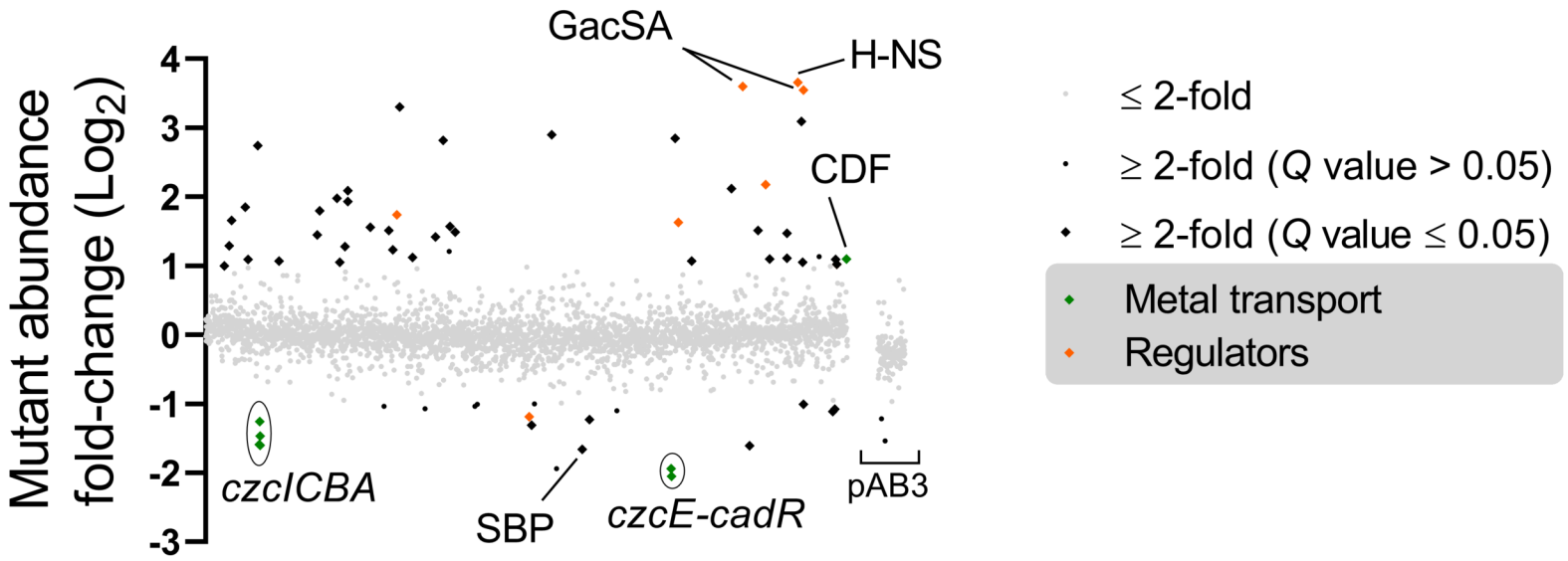
Mutant abundance
fold-change (Log2)
4
3
2
1
0
-1
-2
-3
GacSA
H-NS
CDF
czcICBA
SBP
czcE-cadR
pAB3
≤ 2-fold
≥ 2-fold (Q value > 0.05)
≥ 2-fold (Q value ≤ 0.05)
Metal transport
Regulators

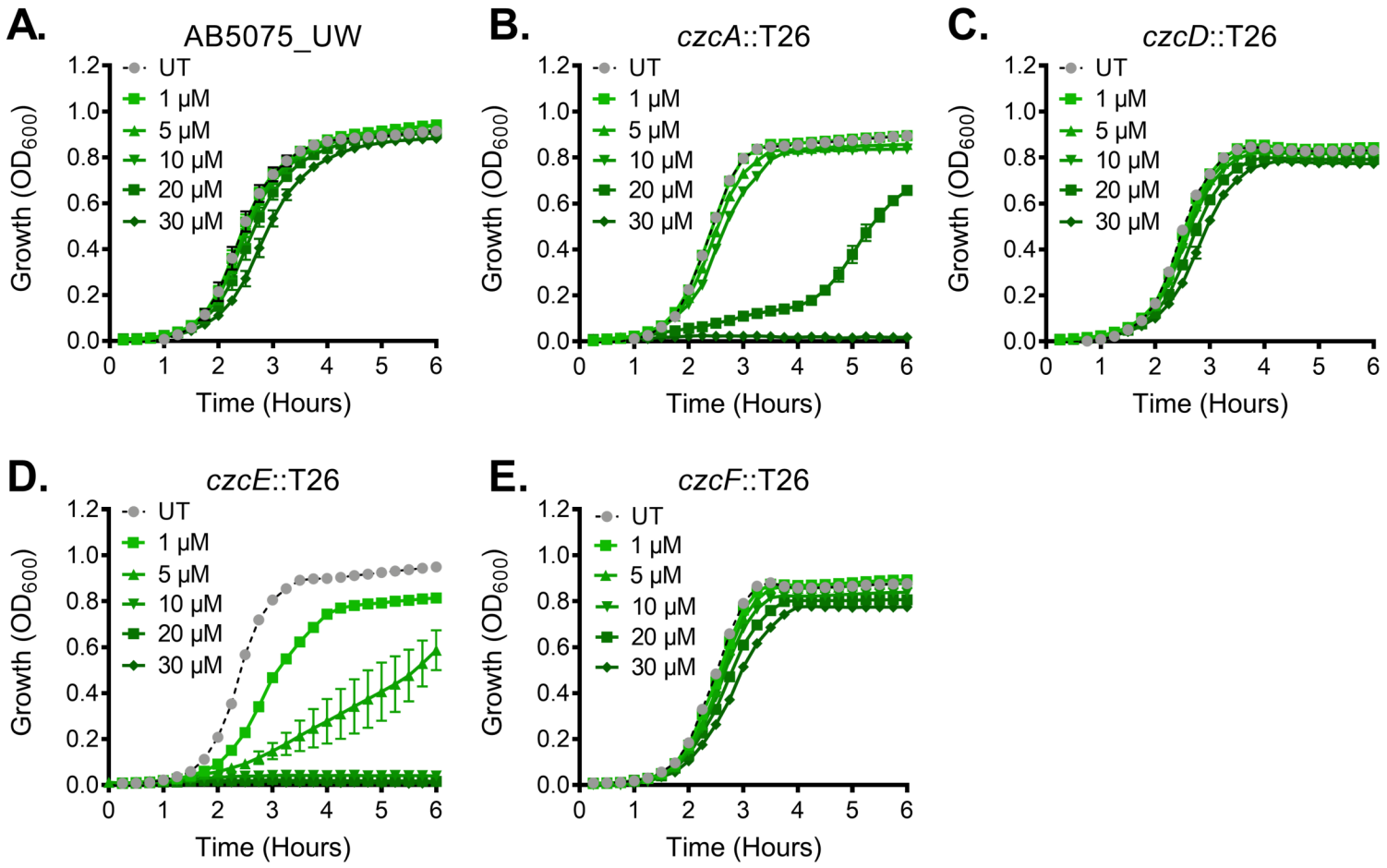
A.
AB5075_UW
B.
czcA::T26
C.
czcD::T26
D.
czcE::T26
E.
czcF::T26
UT
1 μM
5 μM
10 μM
20 μM
30 μM
Growth (OD600)
Time (Hours)
0.0
0.2
0.4
0.6
0.8
1.0
1.2
0
1
2
3
4
5
6

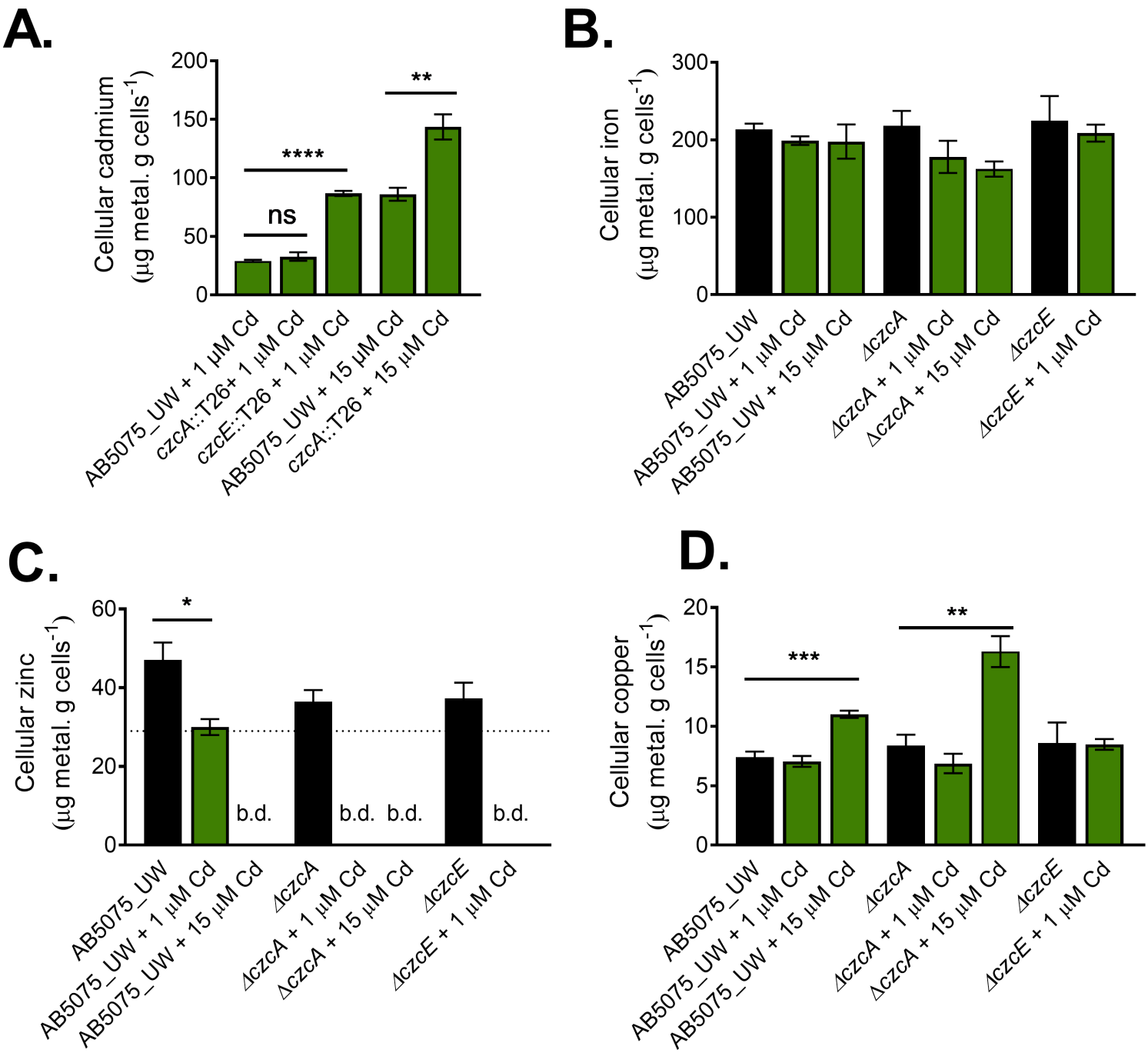
A.
Cellular cadmium
(µg metal. g cells-1)
200
150
100
50
0
****
ns
**
AB5075_UW + 1 µM Cd
czcA::T26+ 1 µM Cd
czcE::T26 + 1 µM Cd
AB5075_UW + 15 µM Cd
czcA::T26 + 15 µM Cd
B.
Cellular iron
(µg metal. g cells-1)
300
200
100
0
AB5075_UW
AB5075_UW + 1 µM Cd
AB5075_UW + 15 µM Cd
ΔczcA
ΔczcA + 1 µM Cd
ΔczcA + 15 µM Cd
ΔczcE
ΔczcE + 1 µM Cd
C.
Cellular zinc
(µg metal. g cells-1)
60
40
20
0
*
b.d.
b.d.
b.d.
b.d.
AB5075_UW
AB5075_UW + 1 µM Cd
AB5075_UW + 15 µM Cd
ΔczcA
ΔczcA + 1 µM Cd
ΔczcA + 15 µM Cd
ΔczcE
ΔczcE + 1 µM Cd
D.
Cellular copper
(µg metal. g cells-1)
20
15
10
5
0
***
**
AB5075_UW
AB5075_UW + 1 µM Cd
AB5075_UW + 15 µM Cd
ΔczcA
ΔczcA + 1 µM Cd
ΔczcA + 15 µM Cd
ΔczcE
ΔczcE + 1 µM Cd

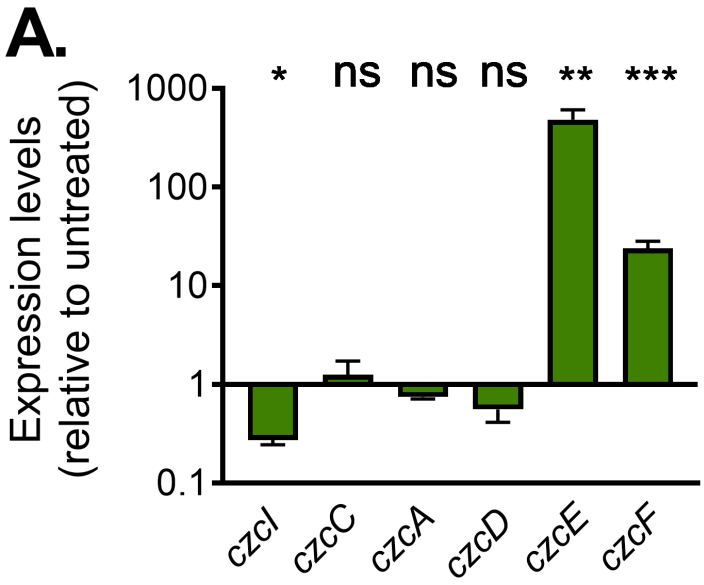
A.
Expression levels
(relative to untreated)
1000
100
10
1
0.1
*
ns
ns
ns
**
***
czcI
czcC
czcA
czcD
czcE
czcF

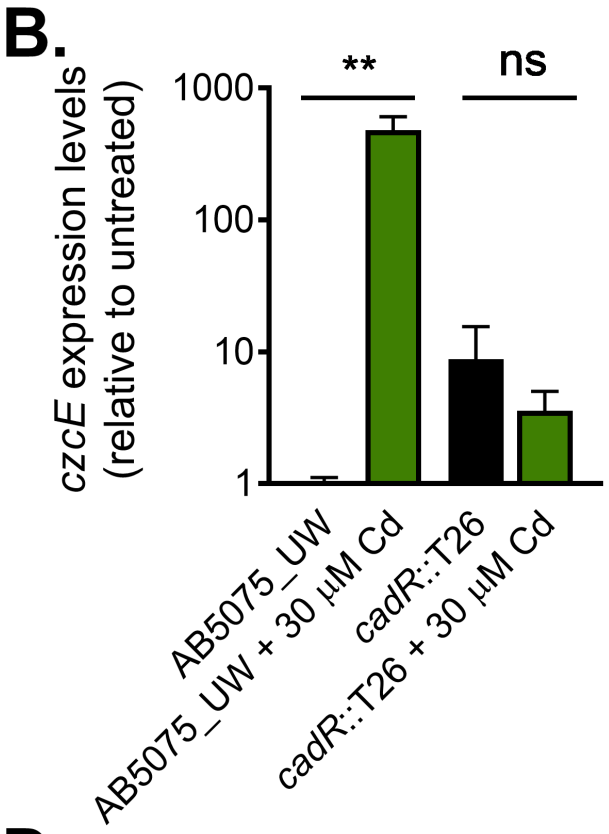
B.
czcE expression levels
(relative to untreated)
1000
100
10
1
**
ns
AB5075_UW
AB5075_UW + 30 μM Cd
cadR::T26
cadR::T26 + 30 μM Cd

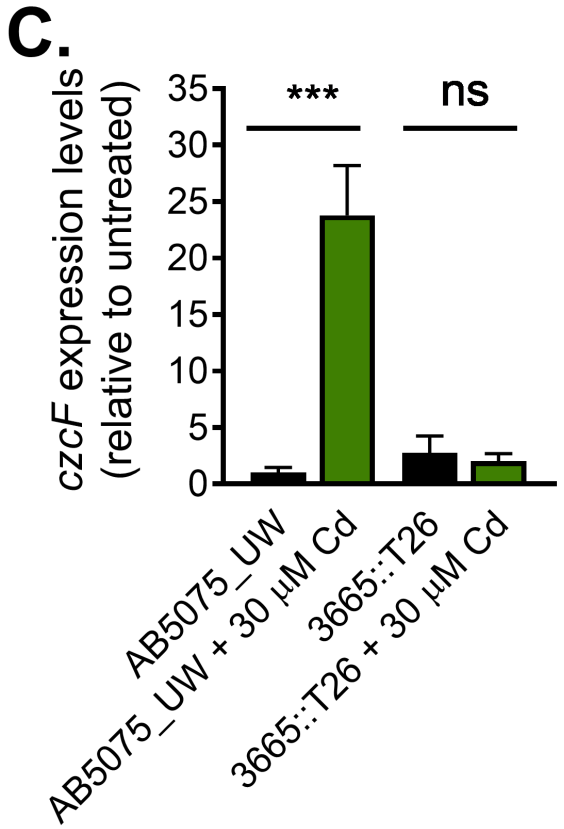
C.
czcF expression levels
(relative to untreated)
35
30
25
20
15
10
5
0
***
ns
AB5075_UW
AB5075_UW + 30 μM Cd
3665::T26
3665::T26 + 30 μM Cd

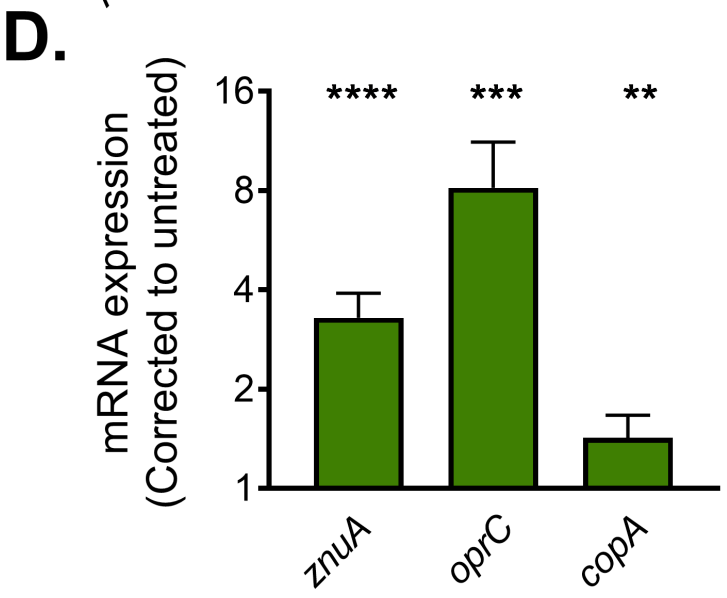
D.
mRNA expression
(Corrected to untreated)
16
8
4
2
1
****
***
**
znuA
oprC
copA